# OPTIMIZATION OF HIGH PRESSURE COLD SPRAY PARAMETERS BASED ON RESPONSE SURFACE MODEL AND GENETIC ALGORITHM

Wenjie HU[1,2,*], Oleksandr SHORINOV[2]

*With the development of computer technology, more and more engineering fields require computers. This paper introduces the response surface method (RSM) and genetic algorithm (GA) into the cold spray technology field to solve the problem of difficulty in injecting powder under high pressure. For the first time, a helical powder feed structure is introduced. The CFD numerical simulation of the supersonic movement trajectory of titanium alloy particles under high pressure conditions is used to study the influence of parameters on the exit particle velocity of high-pressure cold spraying. The multi-parameter optimization of aviation titanium alloy particle acceleration characteristics using the RSM method is established, with a mathematical parameter regression equation of three factors and three levels of injection angle, throat size, and inlet pressure. Further, the genetic algorithm is used for comparative analysis. The results show that the optimized parameters obtained by the response surface method are injection angle of 90°, throat size of 2.35mm, and inlet pressure of 6MPa, with the maximum particle velocity of 858.48m/s, which can meet the needs of various particle deposition. After verification, the error value is 3%. The optimized parameters obtained by the genetic algorithm are injection angle of 90°, inlet pressure of 6MPa, and throat size of 3mm, with the exit collision velocity of 790m/s. After verification, V = 820m/s, with an error of 3.7%.*

**Keywords**: Computer technology, Cold spraying technology, Titanium alloy, RSM, Genetic algorithm

## 1. Introduction

With the development of computer technology, more and more fields have applied computer technology, especially in engineering applications, like relying on numerical simulation to predict results, mainly to reduce waste of experimental resources. For example, in the field of cold spraying, computer 3D modeling software (SolidWorks[1]), computer fluid dynamics software (CFD[2-3], CFX[4]) flow field analysis, computer simulation particle deposition software (abaqus[5-7],

[1] School of Aeronautics and Astronautics, Nanchang Institute of Technology, Nanchang, China, 837406613@qq.com
[2] Department of Aircraft Engines, National Aerospace University "Kharkiv Aviation Institute", Kharkiv, Ukraine.

and lammps [8]), computer multi-physical field analysis software (Comsol) and multi-parameter analysis software (Design-expert and matlab[9]) have been applied.

Cold spraying technology is a new type based on the rational utilization of aerodynamic principles. It is a compressed gas preheated by a heating facility, generating high-speed airflow through a scaled Laval nozzle. The sprayed powder particles are fed into the airflow along the axis, and after being accelerated by the gas, they collide with the substrate at high speed, causing severe plastic deformation and depositing a coating onto the substrate. Because the temperature of the powder particles during the entire deposition process is lower than their melting point, it is called cold spraying [10-11]. In the actual cold spraying process, typical working gases are $N_2$, He, and air, as well as a mixture of gases formed in a certain proportion. The preheating temperature of the working gas is generally less than 600 ℃. In addition, cold spraying technology is a solid-state deposited titanium alloy protective coating, which has high bonding strength and good impact toughness. Therefore, using cold spraying is a good way to solve the surface deposition problem of titanium alloys [12-16]. In addition, cold spray additive manufacturing is still in the theoretical exploration stage [17]. For high-pressure cold spraying, if a positive pressure channel is used to inject titanium alloy powder, for high-pressure cold spraying, the powder channel needs to be given a certain pressure to assist injection, which not only causes turbulence inside the nozzle but also powder bonding. In addition, the parameters of cold spraying technology are complex, and the parameters of high-pressure cold spraying can be referenced from those of low-pressure cold spraying, so as the work [18] indicates that the main parameters affecting deposition include spraying distance, powder properties, gas properties, etc. The key structure of cold spraying is the noise [19-21], and the key to the noise is the throat parameter [1]. However, the above work is all low-pressure cold spraying, so it is necessary to study high-pressure cold spraying.

This paper is the first time to introduce a spiral injection structure to solve the problem of high-pressure powder injection. Then use computer technology to explore the rules of parameters of high pressure, and further optimize the parameters of high-pressure cold spraying. Cold spraying is one of the advanced manufacturing technologies, that incurs significant experimental costs without computer simulation, and numerical simulation can effectively save costs. To study the influencing parameters of high-pressure cold spraying, in this paper, the CFD numerical simulation is used to track the trajectory of titanium alloy particles, and RSM and GA are used to conduct a study on the influencing parameters of the outlet particle velocity in high-pressure cold spraying.

## 2. Cold spray nozzle model and single factor analysis

In this chapter, the simulation process uses the SolidWorks fluid simulation module. The propellant gas in the simplified nozzle is an ideal inviscid gas without heat exchange with the outside world, and its flow can be regarded as a steady-state isentropic flow.

### 2.1 3D modeling

The powder injection port and the main airflow channel should be set separately for 3D preliminary modeling. The exit is a powder and airflow mixing channel. The connection between the injection port and the main airflow channel adopts an anti-air flow reverse structure. The granular material 5 enters the material filling device through the feeding port 3, transmits the granular material 5 forward through the motor 2 or the hand wheel rocker 1 in the material quantitative conveying section 4, the material conveying section 4 squeegees the transmitted granular material 5, and the check valve 6 produces a force on the granular material 5, squeegees the granular material 5 and compacts the granular material 5, when the granular material 5 is squeezed to a certain density, The thrust generated by pushing the granular material 5 is greater than the thrust of the air pressure on the check valve 6, the check valve 6 is opened, and the granular material 5 is pushed into the pressure pipeline; After the granular material 5 pushed into the pressure pipeline is blown away by the airflow in the pressure pipeline, the check valve 6 is pushed by the airflow to complete the seal, preventing the airflow in the pressure pipeline from returning. As shown in Fig. 1.

Using 3D for preliminary modeling, it is necessary to set up a powder injection port and a main airflow channel. The outlet is a powder and airflow mixing channel. The connection between the injection port and the main airflow channel adopts an anti-air flow reverse structure. The spiral powder injection structure can achieve electric and manual dual-function characteristics. The specific operation process is as follows: Particle material 5 enters the material filling device through the feeding port 3 and is transported forward in the material quantitative conveying section 4 through the motor 2 or the hand wheel rocker 1. The material conveying section 4 squeezes and transmits the particle material 5, and the check valve 6 exerts a force on the particle material 5 to compact it. When the particle material 5 is squeezed to a certain density, the thrust generated by pushing the particle material 5 is greater than the air pressure on the check valve. With a thrust of 6, check valve 6 opens and particulate material 5 is pushed into the pressure pipeline; After the particle material 5 pushed into the pressure pipeline is blown away by the airflow in the pressure pipeline, check valve 6 is pushed by the airflow to complete the sealing, preventing the airflow from flowing back in the pressure pipeline. As shown in Fig. 1.

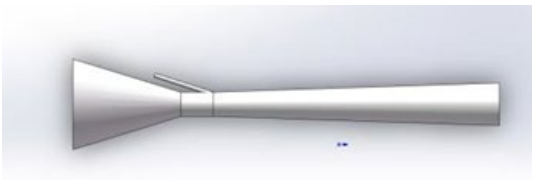

(a) Overall 3D diagram

(b) spiral structure

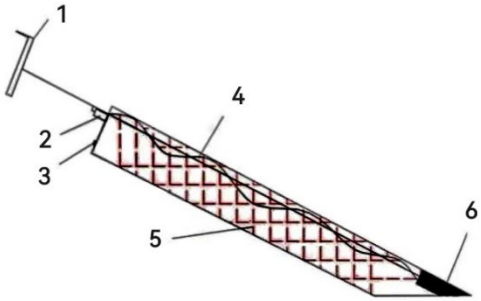


(c) Spiral structure component diagram

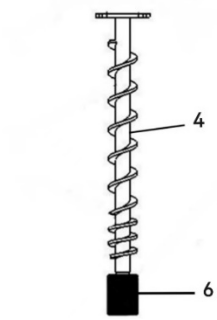


(d) Internal diagram of spiral structure

Fig. 1. 3D model

### 2.2 Factorial analysis of CFD numerical simulation

Low thermal conductivity, low heat loss from gas flow, and particles for nozzle materials are beneficial for increasing particle velocity, but excessive temperature can lead to throat blockage [22-23]. The position of powder injection is shown in Fig. 2.

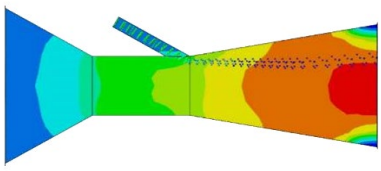

(a)30°

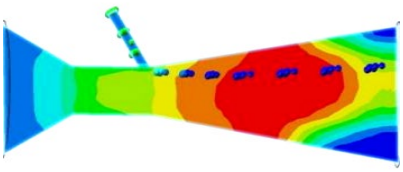

(b)60°

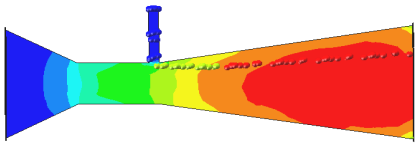

(c)90°

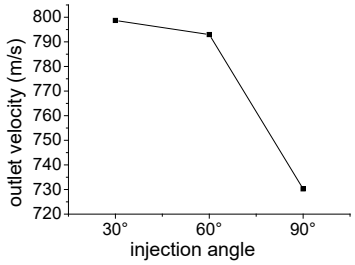


(d)Relation between injection Angle and particle velocity

Fig. 2. Throat size(6mm) and different injection angle

To achieve the injection of powder with a spiral structure and facilitate numerical simulation, the structure was simplified by using a powder outlet pressure slightly higher than the main channel pressure. The effects of injection angle, inlet pressure, and throat size on the velocity of cold spray particles were analyzed. Three key technical parameters were analyzed: a throat size of 6mm, different injection angles (30°, 60°, 90°), the same injection angle with different throat sizes (1mm, 3mm, 6mm), and a throat size of 3mm with different pressures (2MPa, 3MPa, 5MPa), the pressure outlet is one atmosphere. The trajectory of the particle is shown in Fig. 2-Fig. 4.

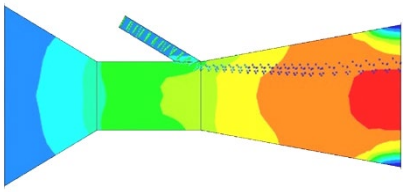

(a)1mm

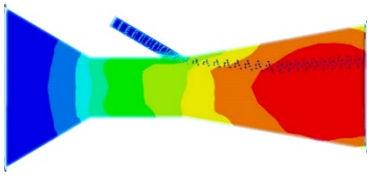

b)3mm

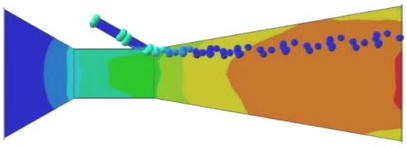

(c)6mm

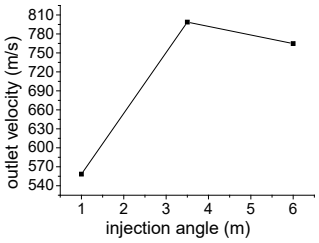


(d)Relation between throat size and particle velocity

Fig. 3. Injection angle(30°) and different throat size

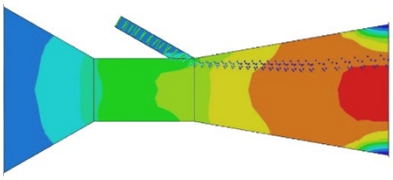

(a)1MPa

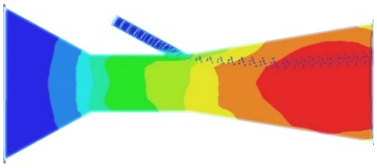

(b)3.5MPa

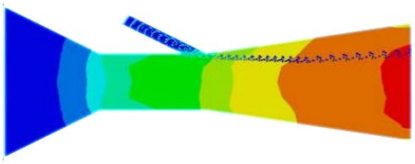

(c)6MPa

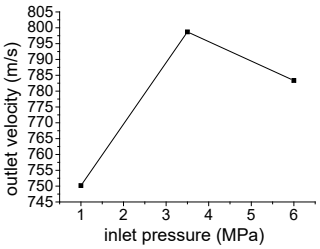


(d)Relation between inlet pressure and particle velocity

Fig. 4. Throat size(3mm) and different pressure

According to the single-factor analysis, the powder injection angle, nozzle throat size, and injection pressure all affect the particle outlet velocity, and all show a certain linear relationship. From Fig. 2(d), Fig. 3(d), and Fig. 4(d), it can be seen that the nozzle throat has the greatest impact on the particle exit velocity, ranging from 1-6mm, with a maximum and minimum difference of 240.37m/s. The injection angle and injection pressure have an impact of 68.4348.51m/s and 48.51m/s, respectively. These results show that cold spraying nozzle throat size is the key parameter of high-pressure cold spraying, which is consistent with the key influence parameters of low-pressure cold spraying.

## 3. Optimization results and discussion

### 3.1 RSM model analysis

In this paper, Design expert software is used for RSM analysis. RSM is a product of combining mathematical and statistical methods, which are widely used in multi-parameter systems [24-25]. Design expert software provides a three-dimensional map, and the analysis results are very intuitive. This paper set injection angle, throat size, and pressure as independent variables and the particle outlet as the dependent variable. The model is represented by equation (1).

$$\mathbf{y} = \beta_0 + \sum_{\mathbf{i}=1}^{\mathbf{m}} \beta_{\mathbf{i}} \mathbf{x}_{\mathbf{i}} + \sum_{\mathbf{i}=1}^{\mathbf{m}} \beta_{\mathbf{ij}} \mathbf{x}_{\mathbf{j}} + \sum_{\mathbf{i}=1}^{\mathbf{m}} \beta_{\mathbf{ii}} \mathbf{x}_{\mathbf{i}}^{\mathbf{2}} + \varepsilon \quad (1)$$

Where $\mathbf{y}$ is the response value of the regression equation, $X_{\mathbf{i}}$ and $X_{\mathbf{j}}$ are independent variables; m is the number of independent variables, and $\beta_0$ is intercept of regression ; $\beta_{\mathbf{i}}$ , $\beta_{\mathbf{ij}}$ and $\beta_{\mathbf{ii}}$ are the regression coefficient of $X_{\mathbf{i}}$, $X_{\mathbf{j}}$; $\varepsilon$ is a random error.

By completing 16 sets of results and conducting an analysis of variance (Table 1), a mathematical model can be obtained, as shown in Equation (2).

*Table 1*

**Model data analysis**

| Source | Squares | df | Square | Value | Prob > F |
|---|---|---|---|---|---|
| Model | 97591.23 | 9 | 10843.47 | 5.22 | 0.0202 |
| A-Injection Angle | 1034.9 | 1 | 1034.9 | 0.5 | 0.5032 |
| B-Throat Size | 14321.94 | 1 | 14321.94 | 6.89 | 0.0341 |
| C-Gas P | 20957.19 | 1 | 20957.19 | 10.08 | 0.0156 |
| AB | 10137.47 | 1 | 10137.47 | 4.88 | 0.0629 |
| AC | 1222.9 | 1 | 1222.9 | 0.59 | 0.4681 |
| BC | 18020.38 | 1 | 18020.38 | 8.67 | 0.0216 |
| A2 | 1854.85 | 1 | 1854.85 | 0.89 | 0.3762 |

| | | | | | |
|---|---|---|---|---|---|
| B2 | 27963.08 | 1 | 27963.08 | 13.46 | 0.008 |
| C2 | 545.88 | 1 | 545.88 | 0.26 | 0.6241 |
| Residual | 14546.8 | 7 | 2078.11 | | |
| Lack of Fit | 14546.8 | 3 | 4848.93 | | |
| Pure Error | 0 | 4 | 0 | | |
| Cor Total | 112100.00 | 16 | | | |

The F value in the model is 5.22, and the P value is 0.0202, which is less than 0.05, indicating that the model is feasible. Establish a particle velocity model, and the particle velocity as formula (2) show.

$$V_P = 793.13 + 11.37A + 42.31B + 51.18C - 50.34AB + 17.5AC - 67.12BC - 21A^2 - 81.5B^2 - 11.39C^2 \quad (2)$$

Based on the contour analysis in Fig. 5, the impact of throat size factors is greater than that of inlet pressure, and the impact of inlet pressure factors is greater than that of injection angle. Therefore, for structural development, the focus should be on the throat size, and other parameters also need to be considered comprehensively to achieve the optimal effect.

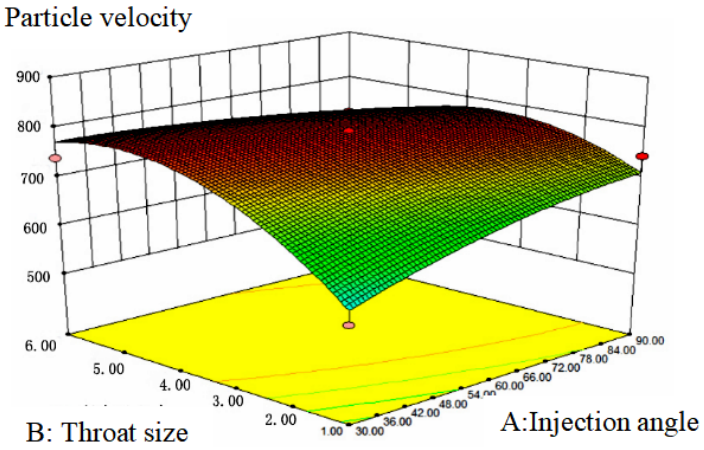


(a)interaction effect of injection angle and throat

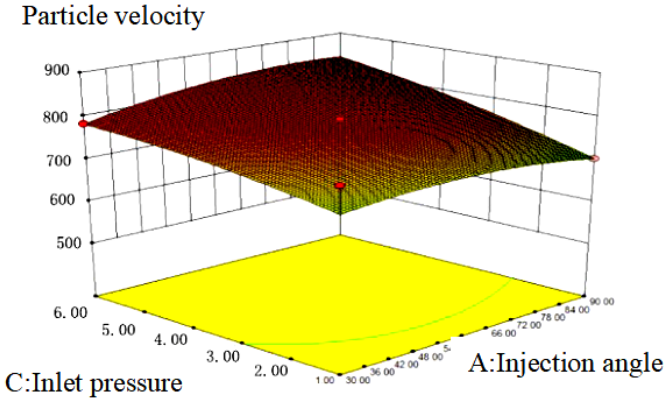


(b) Interaction effect of injection angle and inlet pressure

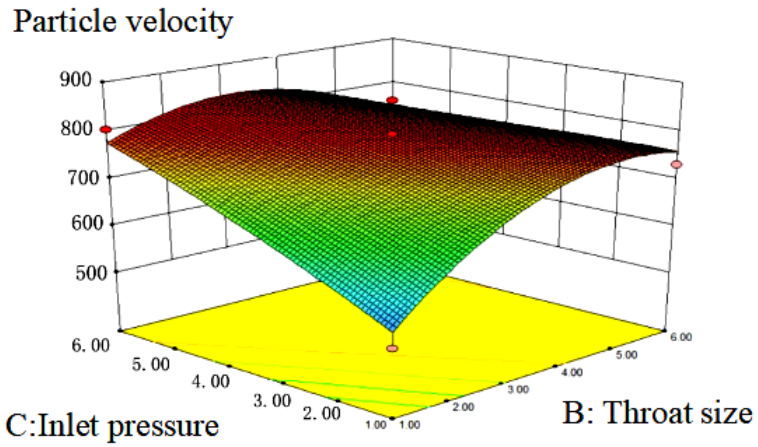


(c)The interaction effect of throat size and inlet pressure.

Fig. 5. The interaction effect of three factors

With the maximum outlet velocity as the ultimate goal, the established mathematical model is used to optimize the parameters. As shown in Fig. 6, the optimal parameters are injection angle = 90° , throat size = 2.35mm, and inlet pressure value = 6mm, which can achieve an outlet velocity of 858m/s. The actual value is verified by numerical simulation to be 832m/s (Fig. 7), with an error value of 3%, indicating high accuracy and a reliable model.


(a)The injection angle(90°)

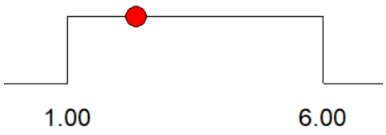


(b) The throat size(2.35mm)


(c) The inlet pressure(6MPa)

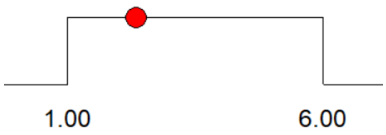


(d) Powder impact velocity(v=858.121m/s)

Fig. 6. The optimal parameter of collision velocity using N2.

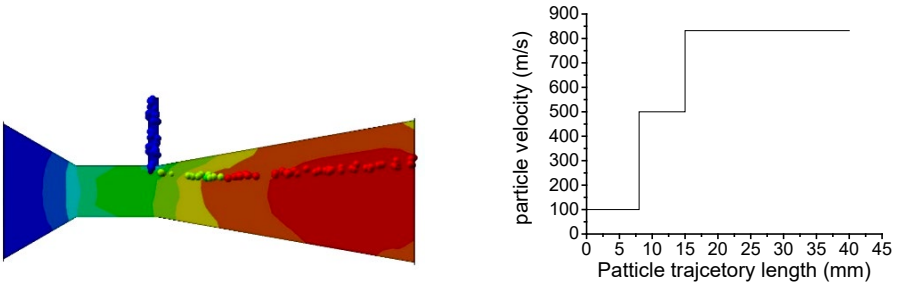


(a) Paticles trajactory

(b) The velocity of particles changing with their motion trajectory

Fig. 7. Powder impact velocity and motion trajectory after optimizing

### 3.2 BP neural network+genetic algorithms analysis

Neural networks and genetic algorithms are widely used in the field of engineering [26-29], which can use Matlab software to get optimized results. The optimal values of particles obtained by further enriching the three key parameters using neural networks and genetic algorithms are obtained by using Latin hypercube sampling to obtain 30 sets of samples, obtaining numerical results for each set of samples, recording the data, and listing them. Among them, 24 sets are used for training the BP neural network, and the remaining 6 sets are used for prediction. The injection angle (X1), throat size (X2), and pressure (X3) ranges are 30° -90° , 1mm-6mm, and 1MPa-5MPa, respectively. Different types of units can be encoded using the following simple formulas (3)-(5), respectively. To facilitate the acquisition of particle exit velocity, the input parameters are rounded to one decimal place or rounded to the nearest integer. The sampling data table is shown in Table 2.

$$y_1 = 60 \times X_1 + 30 \tag{3}$$

$$y_2 = 5 \times X_2 + 1 \tag{4}$$

$$y_3 = 4 \times X_3 + 1 \tag{5}$$

*Table 2*

**Latin hypercube sampling(Keep 1 decimal place or round it)**

| | Injection Angle | Throat Size | Gas P | - | Powder $V_{impact}$ |
|---|---|---|---|---|---|
| Input training | 63 | 5.3 | 1.5 | Output training | 720 |
| | 53 | 5.6 | 3 | | 745 |
| | 60 | 2.56 | 2 | | 746 |
| | 90 | 3.6 | 5 | | 790 |
| | 70 | 1.6 | 3 | | 748 |
| | 88 | 2 | 4.5 | | 760 |
| | 61 | 1.3 | 2.5 | | 723 |
| | 55 | 2.9 | 5 | | 757 |

| | | | | | |
|---|---|---|---|---|---|
| | 77 | 2 | 2 | | 742 |
| | 74 | 5.7 | 4. | | 750 |
| | 56 | 2.8 | 1 | | 735 |
| | 38 | 5.3 | 3.5 | | 740 |
| | 39 | 4 | 3.5 | | 760 |
| | 79 | 3.2 | 3 | | 752 |
| | 71 | 3 | 2 | | 775 |
| | 33 | 3.8 | 4 | | 761 |
| | 67 | 1 | 2 | | 706 |
| | 73 | 4.5 | 3.5 | | 756 |
| | 42 | 5.1 | 1 | | 721 |
| | 50 | 1.3 | 2 | | 730 |
| | 80 | 4.7 | 3 | | 750 |
| | 45 | 4.2 | 4.5 | | 740 |
| | 82 | 6 | 2 | | 768 |
| | 86 | 2.3 | 4 | | 785 |
| Input prediction | 31 | 5 | 4 | Output prediction | 752 |
| | 52 | 3.4 | 1.5 | | 734 |
| | 47 | 1.7 | 3 | | 730 |
| | 64 | 2.5 | 5 | | 755 |
| | 41 | 4 | 1.5 | | 735 |
| | 36 | 4.6 | 4 | | 763 |

Due to the high accuracy of three-layer neural networks [30], this section defines the injection angle, gas pressure, and throat size as inputs. The particle outlet velocity as the output. The hidden layer neural networks in the middle three layers are analyzed and tested with hidden layer numbers ranging from 7 to 12. The results are shown in Fig. 8. When the number of neurons is 9, the mean square error (MSE) is minimized.

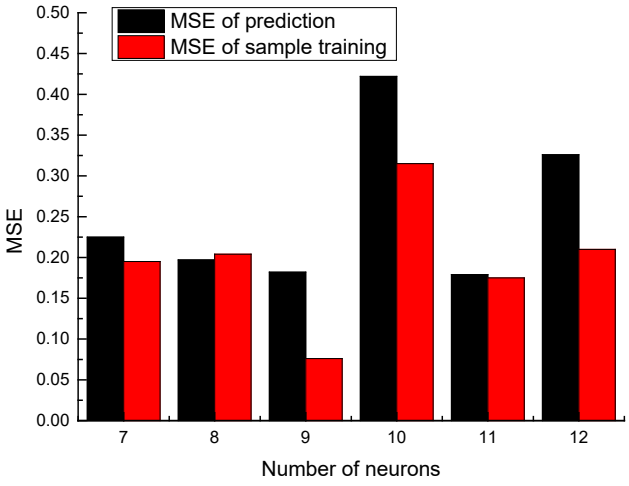


Fig. 8. Mean squared error for different number of neurons

The transfer functions are hyperbolic tangent function (tansig) and linear function (purelin), and the training algorithm is gradient descent. Normalization is applied for different units, and the data is limited to the range of [-1,1]. The normalization expression is shown in formula (6):

$$\mathrm{y_i} = 2 \times \frac{x_i - x_{\min}}{x_{\max} - x_{\min}} - 1 \tag{6}$$

Where, $\mathrm{x_i}$ (i=1, 2,... 30) is the training sample, $X_{\max}$ is the maximum values, and $X_{\min}$ is the minimum values in the training sample, $\mathrm{y_i}$ is the normalized training sample.

The fitness of individuals needs to be determined, as defined in formula (7).

$$\mathrm{fitness} = \frac{1}{M} \sum_{\mathrm{j=1}}^{M} \sum_{\mathrm{i=1}}^{\mathrm{q}} \left(Y_i - T_i\right)^2 \tag{7}$$

In the formula, M is the number of samples, q is the number of output layer neurons, $\mathrm{y_i}$ is the output, and $T_{\mathrm{i}}$ is the expected output. The crossover rate is 0.9, the mutation rate is 0.01, the number of groups is 30, and the maximum iteration number is 200

The parameters optimized by GA are injection angle 90°, air pressure 6MPa, throat size 3mm, and exit collision velocity 790m/s. The numerical method is used to verify V=820m/s with an error of 3.7%. Therefore, neural networks and genetic algorithms (BP+GA) also have good predictive and optimization capabilities for cold spraying process parameters.

## 4. Conclusions and prospects

This paper introduces a spiral injection structure for cold spraying high-pressure environments, aiming at the maximum value of the nozzle outlet, and uses RSM and genetic algorithms to optimize the nozzle outlet velocity of titanium alloy particles for high-pressure cold spraying, obtaining useful conclusions.

1. It is feasible to use response surface methodology (RSM) and genetic algorithms for multi-parameter optimization, with high accuracy. The errors of the two methods are 3% and 3.7%, respectively.

2.It is feasible to inject powder using a spiral structure, and the back-pressure valve is a key structure. The specific beneficial effects of the spiral structure are future research points in the high-pressure environment of cold spraying.

3. Many parameters affect the particle outlet velocity of the high-pressure cold spray nozzle. This paper provides RSM and genetic algorithms to study cold spray parameters but only selects three parameters. Hence, it will be interesting to establish mathematical models for four or more parameters for comprehensive optimization analysis in the future.

**Acknowledgment**

The author would like to thank the China Scholarship Council(NO.202008100011), Science and Technology Research Project of Jiangxi Provincial Department of Education(No. GJJ2202721) and Natural Science Foundation Project of Nanchang Institute of Technology (NLZK-22-05) for its support.

## R E F E R E N C E S

[1]. *Hu W. J, Tan K., Sergii. M., et al*. Study of a Cold Spray Nozzle Throat on Acceleration Characteristics via CFD. Journal of Engineering Sciences, 2021, 8, pp. 19-24.

[2]. *Tang W, Zhang J. Y, Li Y, et al.* Numerical Simulation of the Cold Spray Deposition of Copper Particles on Polyether Ether Ketone (PEEK) Substrate. Journal of Thermal Spray Technology, 2021, 30(7):1792-1809.

[3]. *Chen S.* Study on Influencing Factors of Gas-Particle Two Phase Flow in Cold Spraying Assisted by Electrostatic Field. Henan Polytechnic University.2012.

[4]. *Dolmatov A.I. and Bilchuk O. V.*, Modelling of Gas Flow with Solid Particles in a Short Nozzle, Metallofiz. Noveishie Tekhnol., 40, No. 9: 1257–1271 (2018)(in Russian), DOI: 10.15407/mfint.40.09.1257.

[5]. *Chakrabarty R, Song J.* Numerical simulations of ceramic deposition and retention in metal-ceramic composite cold spray. Surface & Coatings Technology,2020,385125324-125324.

[6*]. Chakrabarty R, Song J.* A modified Johnson-Cook material model with strain gradient plasticity consideration for numerical simulation of cold spray process. Surface & Coatings Technology,2020,397.

[7]. *Ahmed F, Rehan A.* Numerical modelling of particle impact and residual stresses in cold sprayed coatings: A review. Surface and Coatings Technology,2021,409:126835-.

[8]. *Joshi A., James S.,* Molecular dynamics simulation study on effect of process parameters on coatings during cold spray process, Procedia Manuf. 26 (2018) 190–197, https://doi.org/10.1016/J.PROMFG.2018.07.026.

[9]. *Hu W. J, Tan K., Oleksandr S.* Study on Multi-parameter of Cold Spraying Technology via RSM and BP+GA Methods. International Conference on Artificial Intelligence and Advanced Manufacturing, Belgium, Brussels, 2023.

[10]. *Raoelison, R. N., Xie Y, Sapanathan T, et al*. Cold gas dynamic spray technology: a comprehensive review of processing conditions for various technological developments till to date. Addit. Manuf. 2018, 19, 134-159.

[11]. *Assadi H, Gärtner F, Stoltenhoff T, et a1*. Bonding mechanism in cold gas spraying. Acta Materialia, 2003, 51: 4379—4394.
[12]. *Li W. Y., Cao C. C., Yin S.* Solid-state cold spraying of Ti and its alloys: A literature review. Progress in Materials Science. 2020, 110:1-53.
[13]. *Hu W. J., Markovych S., Tan K., et al*. Surface repair of aircraft titanium alloys by cold spray technology. Aerospace technic and technology. 2020, 3:30-42.
[14]. *Kumar S., Ramakrishna M., Chavan NM et al*. Correlation of Splat State with Deposition Characteristics of Cold Sprayed Niobium Coatings. Acta Materialia, 2017, 130: 177-195.
[15]. *Tang J. R., Zhao Z. P., Cui X. Y*. Microstructure and bioactivity of a cold sprayed rough/porous Ta coating on Ti6Al4V substrate. Sci China Tech, 2020, 63:1-9.
[16]. *Hu W. J., Tan K., Markovych S., et al.* Research on the adhesive property of Al+Ti mixed powder deposited on Ti6Al4V substrate by CS using Abaqus/Explicit. Metallofizika i Noveishie Tekhnologii, 2022, 44(5):613-621.
[17].*Tan K., Markovych S., Hu W. J., et al*. Review of application and research based on cold spray coating materials. Aerospace technic and technology, 2021, 1:47-59.
[18]. *Abdulaziz S. Alhulaifi, Gregory A. Buck*. A simplified approach for the determination of critical velocity for cold spray processes. Journal of thermal spray technology, 2014, 23, pp. 1259–1269.
[19]. *Shorinov O, Volkov A, Anatolii D, et al*. Numerical Simulation of a Modified Nozzle for Cold Spraying, Grabchenko's International Conference on Advanced Manufacturing Processes, InterPartner 2023: Advanced Manufacturing Processes V pp. 571–579.
[20]. *Dolmatov A. I. and Polyviany S. A*. Interaction of Solid Particles from a Gas Stream with the Surface of a Flat Nozzle, Metallophysics and Advanced Technologies, 2021, 43(3), pp. 319-328.
[21]. *Li W Y, Li C J.* Optimal design of a novel cold spray gun nozzle at a limit space. Journal of thermal spray technology, 2005, (14), pp. 391-396.
[22]. *Yin S, Meyer M, Li W. Y. et al.* Gas flow, particle acceleration, and heat transfer in cold spray: A rewiew. Journal of thermal spray technology, (2016).doi: 10.1007/s11666-016-0406-8.
[23]. *Cao C C, Li W Y, Han T P, et al.* Simulation study on effect of cold spray nozzle material on particle. Journal of netshape forming engineering, 2019, Vol. 6, pp. 149-53.
[24]. *Shorinov, O., Dolmatov, A., Polyvian, S., et al.* Optimization of cold spray process parameters to maximize adhesion and deposition efficiency of Ni+Al2O3 coatings. Materials Research Express, 2023, 10 (12)126401. DOI:10.1088/2053-1591/ad11fd.
[25]. *Elaiyarasan, U., Ananthi, N. Sathiyamurthy, S*. Prediction and parametric effect of electrical discharge layering of AZ31B magnesium alloy using response surface methodology-assisted artificial neural network. Bull Mater Sci,2024, 47, 109. DOI: https://doi.org/10.1007/s12034-024-03184-6
[26]. *Zhang W, Zhang Z, Gong X, et al.* Estimation Method of Flow Angle of Large Aircraft based on GA-BP neural Network. Computer simulation,2024,41(01):53-57+102
[27]. *Qifu W, Shuzhi L.* A Prediction Model Analysis of Behavior Recognition Based on Genetic Algorithm and Neural Network. Computational Intelligence and Neuroscience, 2022, 20223552908-3552908.
[28]. *Saghi H, Nezhad S R M, Saghi R, et al.* A comparison between Artificial Neural Network and Genetic Algorithm in Predicting liquid sloshing Parameters. Journal of Marine Science and Application, 2024, 23(02):292-301.

[29]. *Oghene O S S, O. J E, Eguakhide A, et al.* Application of response surface methodology and genetic algorithm in the prediction and optimization of the ductile properties of mild steel weld. Welding International, 2024, 38(2):140-152.
[30]. *Gummadi K, Gribble S, et al.* The Impact of DHT Routing Geometry on Resilience and Proximity. In:Proc. SIGCOMM'03, Aug.2003.